PHYSICAL REVIEW B **79**, 020204(R) (2009)

Nanocluster-associated vacancies in nanocluster-strengthened ferritic steel as seen via positron-lifetime spectroscopy

Jun Xu,[1,*] C. T. Liu,[1,2] M. K. Miller,[1] and Hongmin Chen[3]
[1]*Oak Ridge National Laboratory, P.O. Box 2008, Oak Ridge, Tennessee 37831, USA*
[2]*Department of Materials Science and Engineering, University of Tennessee, Knoxville, Tennessee 37996-2200, USA*
[3]*Department of Chemistry, University of Missouri, Kansas City, Missouri 64110, USA*
(Received 4 October 2008; published 22 January 2009)

Nanocluster-strengthened ferritic alloys are promising as structural materials because of their excellent high-temperature strength and radiation-damage resistance. Recently, Fu *et al.* [Phys. Rev. Lett. **99**, 225502 (2007)] predicted that vacancies play an essential role in the formation and stabilization of nanoclusters in these materials. Positron-lifetime spectroscopy has been used to test this theoretical prediction in a nanocluster-strengthened Fe-based alloy. Nanoclusters (2–4 nm in diameter) containing Ti, Y, and O have been observed in a mechanically alloyed ferritic steel by atom-probe tomography. Vacancy clusters containing four to six vacancies have also been found in this material. In contrast, no vacancy clusters were detected in similar alloys containing no nanoclusters. These results indicate that vacancies are a vital component of the nanoclusters in these alloys.

DOI: 10.1103/PhysRevB.79.020204 PACS number(s): 61.72.−y, 71.20.Gj, 81.07.−b, 71.15.Mb

An interesting finding in the recent study of metallic alloys is the discovery of thermally stable nanoclusters in ferritic alloys prepared by mechanical alloying.[1–4] Atom-probe tomography reveals that these nanoclusters with a size of 2–4 nm in diameter contain mainly Ti, Y, and O atoms, with a composition close to (Ti,Y)O. Mechanical tests indicate that these nanoclusters are responsible for the improvement of creep strength, with a reduction in the creep rate by 6 orders of magnitude at 650–900 °C.[3,5] Furthermore, recent studies show that these nanocluster alloys are very resistant to radiation damage; for instance, nanoclusters in the ferritic alloys remain stable even after extensive heavy-ion bombardment at 300–700 °C.[6,7] These results demonstrate the potential use of these materials in nuclear energy power systems.

It is important to point out that these nanoclusters exhibit ultrahigh thermal stability at elevated temperatures.[1,8–11] First, they showed no appreciable growth in size after extensive exposure to temperatures above 1000 °C. Second, these nanoclusters remain stable at 1400 °C, which is 91% of the melting temperature (T_m) after direct quenching from high temperatures or *in situ* measurements at temperature.[12] These results differ from those observed for conventional particles which grow significantly at temperatures above $0.4T_m$. In order to understand this unusual behavior, Fu *et al.*[13] recently determined the binding energy between solute atoms and point defects in the nanocluster ferritic alloys, using first-principles density-functional theory. Their calculations show a very high binding energy (1.5 eV) between oxygen (O) and vacancy (v) in the body-centered-cubic (bcc) Fe lattice. The binding energy can be further enhanced by attracting nearest-neighboring Ti and Y atoms to v-O pairs, resulting in the formation of large v-O-Ti-Y clusters. The binding energy of O in the clusters reaches 5 eV, which is even higher than that of TiO_2 (4.3 eV).

As predicted from the first-principles calculations, vacancies play an essential role in the formation and thermal stability of stable nanoclusters in the ferritic alloys. Thus, characterization of vacancies becomes vitally important for our understanding of formation mechanism of these nanoclusters. Positron-annihilation spectroscopy is currently the sole technology effective in the analysis of vacancies for Fe-based materials.[14–17] Therefore, positron-lifetime spectroscopy (PLS) was used to characterize the size and concentration of vacancies in Fe-based alloys with and without nanoclusters. Also, in order to investigate the correlation between vacancies and nanoclusters, atom-probe tomography (APT) was used to detect the presence of nanoclusters containing Ti, Y, and O atoms.

Three Fe-based alloys were prepared for this PLS study. The first alloy is referred to as the nanocluster-strengthened (NS) alloy with the nominal composition of Fe-14Cr-3W-0.4Ti-0.25Y_2O_3 (wt %) prepared by mechanical alloying followed by hot extrusion in an evacuated can. This material containing stable nanoclusters was well characterized previously by APT.[1,9,10] The second alloy is referred to as the *cast* alloy, which has the same composition of the NS alloy but was prepared by conventional melting and casting. This material contains no nanoclusters because yttrium oxide added for alloying formed slag floating on the top of the ingot, with essentially no residual O and Y in the ingot. The third alloy is called the powder metallurgy (PM) alloy, which was prepared by internal oxidation of prealloyed Fe-14Cr-3W-0.4Ti powder (without addition of Y_2O_3 powder) at 750 °C in oxygen pressure of 3×10^{-3} Pa. The internally oxidized powder was canned and hot extruded. Both APT and mechanical-property characterization indicate no nanoclusters in this material.

The description of APT measurements can be found in Ref. 6. The atomic coordinates and the elemental identities of atoms in a volume of analysis are determined with a position-sensitive single-atom detector placed at the end of the time-of-flight mass spectrometer. An atom map of a selected volume (with a depth of 4 nm in the box) containing two nanoclusters in the NS alloy heat treated for 1 h at 1000 °C is shown in Fig. 1. The nanoclusters are formed

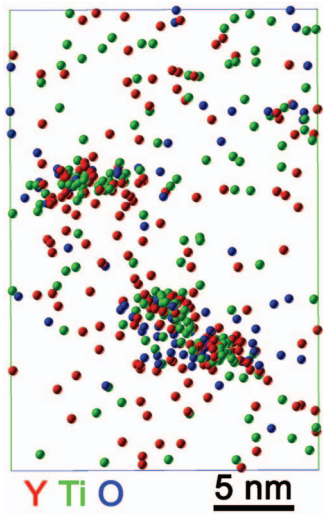

FIG. 1. (Color) Atom map of a selected volume containing 2 nanoclusters in the NS alloy (14YWT). The depth of the volume box is 4 nm. Note that some O atoms are obscured by Ti atoms, as a significant number of TiO ions are detected in this material, and the Ti atom is plotted on top of the O atom.

both in the matrix and on grain boundaries with densities as high as $1\times10^{24}/\mathrm{m}^3$. Stable nanoclusters were not found in the other two alloys: cast and PM.

The NS, cast, and PM alloy samples were analyzed by standard positron-lifetime spectroscopy, which measures the time difference between "birth" radiation and the subsequent annihilation radiation of an individual positron.[17] A fast-fast coincidence positron-lifetime spectrometer with two BaF_2 scintillators having a resolution function of 190 ps full width at the half maximum was used. The radiation source material was 16 μCi ^{22}NaCl enveloped in 5-μm-thick Al foil, which was placed between two identical specimens (sample-source-sample sandwich). Each spectrum contains $2\times10^6-3\times10^6$ single-annihilation events. Lifetime spectra were analyzed using the CONTIN program,[18] which deconvolutes the time spectra into the probability density function (PDF) as a function of positron lifetime via Laplace inversion. A spectrum of ^{207}Bi, which has a known positron lifetime of 182 ps, was used as the reference for CONTIN deconvolution.

The positron-lifetime spectra measured at room temperature for samples of the cast, PM, and nanocluster-embedded NS alloys are shown in Fig. 2. Due to the β^+ decay, the source emits positrons with energy ranging from 0 to 540 keV. As a result, the depth of the samples analyzed is less than 120 μm, determined by $d=40E^{1.6}/\rho$, where d is the mean depth in nanometer, ρ is the density of the material in $\mathrm{g/cm}^3$, and E is the ^{22}Na positron implantation energy in keV. The PDF as a function of positron lifetime, resulting from CONTIN deconvolution of the spectra in Fig. 2 are shown in Fig. 3. For the cast alloy, a dominant lifetime peak was observed centered at 142 ps with the 97% of the total PDF spectrum intensity, as shown in Fig. 3(a). A small broad peak (corresponding to a density of 3%) is observed at 405 ps. Similar results are observed for the PM alloy sample [Fig. 3(b)], which shows a dominant peak at 140 ps with 95% of the spectrum intensity. A small peak was also observed here at ~400 ps. The lifetimes for the cast alloy and the PM alloy are a superposition of the free-positron lifetime (104 ps) (Ref. 17) and monovacancy lifetime (175 ps). These

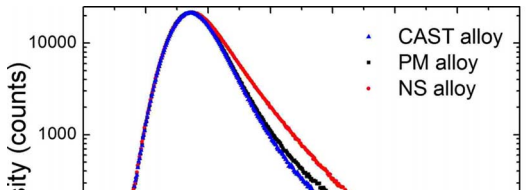

FIG. 2. (Color online) Semilogarithmic plots of the counting rates as a function of the arrival time of annihilation gamma rays for the cast alloy (triangles), the PM alloy (squares), and the NS alloy (circles). The spectra were shifted for the same starting time at 3.26 ns and were normalized for the same height.

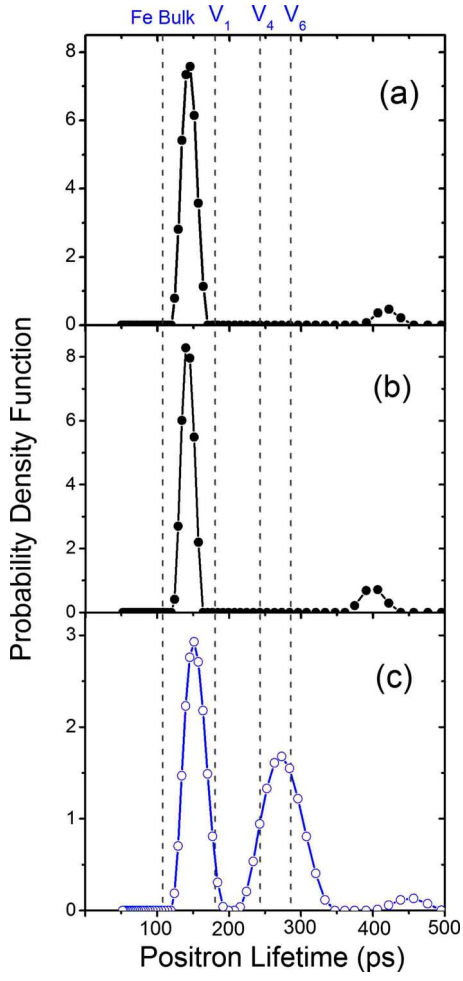

FIG. 3. (Color online) Probability density functions as a function of positron lifetime, resulting from Laplace inversion (CONTIN): (a) cast alloy, (b) PM alloy, and (c) NS alloy. Calculated positron lifetimes for free positrons and positrons being trapped in vacancy clusters in pure Fe are plotted as the dashed lines.

lifetimes are interpreted as a combination of free positrons and those being trapped in the monovacancies. The current experimental and analytical methods cannot separate these two components. The low-intensity long-lifetime component at >400 ps is believed due to an artifact associated with a small sample size (3 mm in diameter) which did not completely cover the source. Such a component was not observed with either the ^{207}Bi reference sample or with larger Fe samples.

The NS alloy samples exhibit a PDF distribution that is distinctly different from that of the cast and PM samples, as shown in Fig. 3(c). The distribution pattern consists of three distinct peaks: $(\tau_1, I_1)=(151\ \text{ps}, 48\%)$, $(\tau_2, I_2)=(273\ \text{ps}, 51\%)$, and the small peak at 450 ps with intensity of 1%. τ_1 and τ_2 are the first two lifetimes and I_1 and I_2 are their corresponding relative intensities. The relative intensities were determined by the ratios of τ_1 and τ_2 peak areas to the total area. Note that the calculated positron lifetimes for different vacancy cluster sizes in pure bcc Fe (Refs. 19 and 20) are also shown as the vertical dashed lines in Fig. 3(c). These lines should only be used as an approximate guide due to the other solutes present in these alloys. There are two possibilities for the $\tau_1=151$ ps component: first is a combination of positron lifetimes for free positrons and positrons being trapped in monovacancies (i.e., the same assignment as for the cast alloy and PM alloy) and second is a positron lifetime due to sole monovacancy complexes, such as vacancy-oxygen pairs. This lifetime is ~10 ps longer than those for the cast and PM alloys. If this lifetime is due to the first possibility, the longer lifetime suggests greater monovacancy concentration in the NS alloy. If this lifetime is due to vacancy-oxygen complexes, the concentration of the complexes is expected to be one order higher.

In Fig. 3(c), the second peak centered at $\tau_2=273$ ps is due to the contributions of positrons being trapped in vacancy clusters having four to six atomic vacancies. It is important to point out that the vacancy cluster component was not observed either for the cast or PM alloy. Because one structural difference between the NS alloy and the other two alloys is the presence of the Y-, Ti-, and O-rich nanoclusters, it is thus reasonable to relate the vacancy clusters to the presence of the nanoclusters in the NS alloy. This correlation suggests that nanoclusters have a strong affinity for vacancies. This correlation is consistent with the theoretical calculations by Fu *et al.*,[13] which indicate strong binding energies between vacancies and solute atoms of O, Ti, and Y. Further verification of these vacancy-solute complexes can be done using coincidence Doppler broadening measurements, as performed by others.[19,20]

Assuming that the positrons are being trapped in monovacancies and vacancy clusters, in addition to the free positrons, the concentrations of monovacancies and vacancy clusters in the NS alloy were estimated with the so-called two-state trapping model.[21] The lifetimes of free positrons and those trapped in monovacancies in Fe are given as 104 and 175 ps, respectively.[21] The lifetime component (τ_1, I_1) is assumed to be the combination of both free positrons and those trapped in monovacancies of the Fe alloy. After considering these factors, the concentrations for monovacancies and vacancy clusters are estimated to be ~30 and ~7 ppm, respectively. Considering five vacancies in each cluster, the total vacancy concentration in the alloy can be thus estimated to be ~65 ppm.

The oxygen concentration in pure Fe is very low, which is on the order of 1 ppm at 900 °C. Because of the strong binding energy of v-O pairs in the bcc Fe lattice, Fu *et al.*[13] predicted that the vacancy concentration can be as high as the oxygen concentration in the NS alloy. In the NS alloy, oxygen can exist in three possible states: O atoms in solid solution with the bcc Fe lattice (including possible v-O pairs), O atoms in the nanoclusters, and O atoms in coarse oxide particles (e.g., TiO_2 and Y_2O_3 particles). In order to determine the oxygen level in the first two regions, the unique capability of atom-probe tomography was used to estimate the O concentration in the matrix plus the nanocluster regions. The average oxygen concentration in these regions is estimated to be 1800 ± 200 ppm.

A large fraction of the oxygen concentration is supposedly equivalent to the vacancy concentration, as suggested by the first-principles calculations.[13] However, the combined concentration of monovacancies and vacancy clusters (65 ppm), obtained from the PLS, is much lower than the estimated oxygen concentration. This discrepancy is most likely due to the assumption of (τ_1, I_1) component as a combination of free positrons and those trapped in monovacancies. If this component is assigned as monovacancy-oxygen pairs (v-O) alone, the concentration of the monovacancy-oxygen complexes should be at least 1 order of magnitude higher than the estimates based on the free-positron–monovacancy combination. Because no calibration is currently available for the lifetime of the monovacancy-oxygen pairs, these concentrations cannot be determined. Furthermore, the size of the vacancy clusters determined by PLS represents a contiguous open volume. However, Y and Ti atoms are significantly larger than Fe atoms and local rearrangements due to relief of local stresses will reduce the extent of the open space. Therefore, the number of vacancies determined by PLS may be underestimated.

In conclusion, the formation of vacancy clusters in cast, PM, and NS ferritic alloys and vacancies associated with the presence of nanoclusters containing Ti, Y, and O atoms has been investigated with positron-lifetime spectroscopy and atom-probe tomography. Vacancy clusters containing equivalently four to six vacancies were found in the NS alloy that contained stable nanoclusters. The concentration of monovacancy complexes and vacancy clusters is estimated to be greater than 30 and 7 ppm, respectively. No vacancy clusters were detected in similar alloys containing no nanoclusters. The observed vacancy clusters are consistent with the prediction that vacancies are necessary for stabilizing nanoclusters formed in the NS alloy.

The authors would like to thank C. L. Fu of ORNL for his helpful discussion. This research was sponsored by the U.S. Department of Energy, Division of Materials Sciences and Engineering. Research at the Oak Ridge National Laboratory SHaRE User Facility was sponsored by the Scientific User Facilities Division, Office of Basic Energy Sciences, U.S. Department of Energy.

*Corresponding author; xuj2@ornl.gov

[1] D. J. Larson, P. J. Maziasz, I.-S. Kim, and K. Miyahara, Scr. Mater. **44**, 359 (2001).
[2] M. K. Miller, D. T. Hoelzer, E. A. Kenik, and K. F. Russell, Intermetallics **13**, 387 (2005).
[3] R. L. Klueh, P. J. Maziasz, I. S. Kim, L. Heatherly, D. T. Hoelzer, N. Hashimoto, E. A. Kenik, and K. Miyahara, J. Nucl. Mater. **307-311**, 773 (2002).
[4] B. Van der Schaaf, F. Tavassoli, C. Fazio, E. Rigal, E. Diegele, R. Lindau, and G. LeMarois, Fusion Eng. Des. **69**, 197 (2003).
[5] R. L. Klueh, J. P. Shingledecker, R. W. Swindeman, and D. T. Hoelzer, J. Nucl. Mater. **341**, 103 (2005).
[6] P. Pareige, M. K. Miller, R. E. Stoller, D. T. Hoelzer, E. Cadel, and B. Radiguet, J. Nucl. Mater. **360**, 136 (2007).
[7] T. R. Allen, J. Gan, J. I. Cole, M. K. Miller, J. T. Busby, S. Ukai, S. Ohtsuka, S. Shutthanandan, and S. Thevuthasan, J. Nucl. Mater. **375**, 26 (2008).
[8] I.-S. Kim, J. D. Hunn, N. Hashimoto, D. J. Larson, P. J. Maziasz, K. Miyahara, and E. H. Lee, J. Nucl. Mater. **280**, 264 (2000).
[9] M. K. Miller, E. A. Kenik, K. F. Russell, L. Heatherly, D. T. Hoelzer, and P. J. Maziasz, Mater. Sci. Eng., A **353**, 140 (2003).
[10] M. K. Miller, R. K. Nanstad, and D. T. Hoelzer, J. Nucl. Mater. **351**, 261 (2006).
[11] J. H. Schneibel, C. T. Liu, D. T. Hoelzer, M. J. Mills, P. Sarosi, T. Hayashi, U. Wendt, and H. Heyse, Scr. Mater. **57**, 1040 (2007).
[12] M. K. Miller, C. T. Liu, and X. L. Wang (unpublished).
[13] C. L. Fu, M. Krcmar, G. S. Painter, and X.-Q. Chen, Phys. Rev. Lett. **99**, 225502 (2007).
[14] M. Eldrup, A. Vehanen, P. J. Schultz, and K. G. Lynn, Phys. Rev. B **32**, 7048 (1985).
[15] T. Toyama, Y. Nagai, Z. Tang, M. Hasegawa, A. Almazouzi, E. van Walle, and R. Gerard, Acta Mater. **55**, 6852 (2007).
[16] H. F. M. Mohamed, J. Kwon, Y.-M. Kim, and W. Kim, Nucl. Instrum. Methods Phys. Res. B **258**, 429 (2007).
[17] M. J. Puska, J. Phys.: Condens. Matter **3**, 3455 (1991).
[18] R. B. Gregory, Nucl. Instrum. Methods Phys. Res. A **302**, 496 (1991).
[19] J. Xu, J. Moxom, B. Somieski, C. W. White, A. P. Mills, Jr., R. Suzuki, and S. Ishibashi, Phys. Rev. B **64**, 113404 (2001).
[20] H. Ohkubo, Z. Tang, Y. Nagai, M. Hasegawa, T. Tawara, and M. Karatini, Mater. Sci. Eng., A **350**, 95 (2003).
[21] A. Vehanen, P. Hautojarvi, J. Johansson, J. Yli-Kauppila, and P. Moser, Phys. Rev. B **25**, 762 (1982).